UDC 621.314 https://doi.org/10.20998/2074-272X.2025.2.05

N. Hadjidj, M. Benbrahim, D. Ounnas, L.H. Mouss

Global maximum power point tracking method for photovoltaic systems using Takagi-Sugeno fuzzy models and ANFIS approach

Introduction. *A new global maximum power point tracking (GMPPT) control strategy for a solar photovoltaic (PV) system, based on the combination of Takagi-Sugeno (T-S) fuzzy models and an ANFIS, is presented. The* ***novelty*** *of this paper lies in the integration of T-S fuzzy models and the ANFIS approach to develop an efficient GMPPT controller for a PV system operating under partial shading conditions.* ***Purpose****. The new GMPPT control strategy aims to extract maximum power from the PV system under varying weather conditions or partial shading.* ***Methods****. An ANFIS algorithm is used to determine the maximum voltage, which corresponds to the actual maximum power point, based on PV voltage and current. Next, the nonlinear model of the PV system is employed to design the T-S fuzzy controller. A reference model is then derived based on the maximum voltage. Finally, a tracking controller is developed using the reference model and the T-S fuzzy controller. The stability of the overall system is evaluated using Lyapunov's method and is represented through linear matrix inequalities expressions. The* ***results*** *clearly demonstrate the advantages of the proposed GMPPT-based fuzzy control strategy, showcasing its high performance in effectively reducing oscillations in various steady states of the PV system, ensuring minimal overshoot and a faster response time. In addition, a comparative analysis of the proposed GMPPT controller against conventional algorithms, such as Incremental Conductance, Perturb & Observe and Particle Swarm Optimization, shows that it offers a fast dynamic response in finding the maximum power with significantly less oscillation around the maximum power point.* References 20, tables 3, figures 14.
Key words: **photovoltaic system, maximum power point tracking, Takagi-Sugeno fuzzy model, linear matrix inequalities.**

Вступ*. Представлена нова глобальна стратегія відстеження точки максимальної потужності (GMPPT) для сонячної фотоелектричної (PV) системи, заснована на комбінації нечітких моделей Такагі-Сугено (T-S) і ANFIS.* ***Новизна*** *статті полягає в інтеграції нечітких моделей T-S і підходу ANFIS для розробки ефективного контролера GMPPT для PV системи, що працює в умовах часткового затінення.* ***Мета****. Нова стратегія контролю GMPPT спрямована на отримання максимальної потужності від PV системи за змінних погодних умов або часткового затінення.* ***Методи****. Алгоритм ANFIS використовується для визначення максимальної напруги, яка відповідає фактичній точці максимальної потужності, на основі PV напруги та струму. Далі нелінійна модель PV системи використовується для розробки нечіткого контролера T-S. Потім на основі максимальної напруги виводиться еталонна модель. Нарешті, контролер стеження розроблено з використанням еталонної моделі та нечіткого контролера T-S. Стійкість системи в цілому оцінюється за допомогою методу Ляпунова і представляється у вигляді лінійних матричних нерівностей.* ***Результати*** *чітко демонструють переваги запропонованої стратегії нечіткого керування на основі GMPPT, демонструючи її високу продуктивність щодо ефективного зменшення коливань у різних сталих станах PV системи, забезпечуючи мінімальне перерегулювання та швидший час відгуку. Крім того, порівняльний аналіз пропонованого контролера GMPPT із звичайними алгоритмами, такими як Incremental Conductance, Perturb and Observe та Particle Swarm Optimization, показує, що він пропонує швидку динамічну реакцію у пошуку максимальної потужності зі значно меншими коливаннями навколо точки максимальної потужності.* Бібл. 20, табл. 3, рис. 14.
Ключові слова: **фотоелектрична система, відстеження точки максимальної потужності, нечітка модель Такагі-Сугено, лінійні матричні нерівності.**

Introduction. Fossil energy has several drawbacks, such as environmental pollution, climate change contributions, and resource depletion. In contrast, renewable energy, like solar and wind power, offers advantages like reduced environmental impact, sustainability, and the potential for job creation and innovation in clean energy technologies. Photovoltaic (PV) solar energy offers compelling advantages. It is a clean and sustainable source with zero emissions, reducing environmental impact. Moreover, solar modules are durable, low-maintenance, and cost-effective over their long lifespan. Scalability makes PV systems versatile for diverse applications, from homes to large-scale projects. Abundant sunlight in many regions promotes energy independence, diminishing reliance on finite resources. Ongoing technological advancements further enhance efficiency and affordability, making PV solar an increasingly attractive and accessible choice for renewable energy [1, 2].

The PV system consists of solar modules that transform sunlight into DC electricity and a DC-DC converter, which plays a pivotal role by facilitating the efficient power transfer from the solar modules to the load. Its primary function is to match the varying voltage levels between the PV module and the load or storage system [3]. In essence, it optimizes power extraction from the solar modules by maintaining the output voltage at the maximum power point V_{mpp} a task typically controlled by the Maximum Power Point Tracking (MPPT) algorithm [4, 5].

Many conventional MPPTs methods have been proposed in the literature, these include Perturb and Observe (P&O) [6, 7], Incremental Conductance (InCond) [8, 9] and Hill Climbing [10]. However, each method has its application challenges and inherent disadvantages. For instance, P&O is susceptible to oscillations around the maximum power point and may result in power losses, especially under rapidly changing irradiance conditions. InCond, while more efficient, can exhibit sensitivity to noise and instability. Hill Climbing methods may struggle in partially shaded conditions and exhibit slow convergence to the optimal operating point.

Additionally, these conventional MPPT approaches may not fully exploit the potential of PV systems under dynamic environmental conditions. As a result, exploring advanced and adaptive MPPT techniques becomes crucial to overcoming these limitations and improving overall performance [11]. On the other hand, shading introduces multiple peaks and valleys in the power-voltage characteristic, leading to inaccurate MPPT operation. These conventional methods may experience slow

convergence and oscillations and may even be trapped in local maximum power points, resulting in sub-optimal energy harvesting. To address these limitations, advanced MPPT techniques, often incorporating intelligent algorithms and adaptive strategies, are increasingly explored to enhance performance in partial shading conditions [12].

Over the past few years, numerous fuzzy MPPT controllers have been suggested, leveraging Takagi-Sugeno (T-S) fuzzy models [13, 14]. The fundamental concept behind T-S fuzzy models is to represent a process by aggregating linear models, facilitating the construction of fuzzy controllers using a technique called parallel-distributed compensation (PDC) [15]. Determination of fuzzy controller gains is dependent on the stability conditions of the augmented T-S fuzzy system, which can be readily formulated as linear matrix inequalities and efficiently solved through convex optimization techniques. In [16] the InCond algorithm is utilized to ascertain the reference voltage. Subsequently, it is combined with a T-S MPPT-based fuzzy controller. Other studies, such as [17], calculated the reference voltage employing a T-S reference model incorporating, as inputs measurements of temperature and irradiation. An alternative approach involves, an MPP searching algorithm, which evaluates the changing levels of irradiation and temperature. This algorithm instantly calculates the partial power derivative which respect to the PV cell current and generates the reference state required for tracking with a PDC controller.

Purpose. This work aims to design a Global Maximum Power Point Tracking (GMPPT) controller using the adaptive ANFIS technique to accurately track the global maximum power point in the presence of partial shading. ANFIS uses PV current and PV voltage as inputs to generate the maximum voltage. Subsequently, a T-S fuzzy controller ensures maximum energy transmission, enhancing the PV system's efficiency. The efficacy of the proposed T-S fuzzy method is assessed through the total-cross-tied configuration, partial shading as well as under sudden solar irradiance changes.

PV system modeling. As seen in Fig. 1, the PV system under consideration is made up of a PV panel, a DC/DC boost converter, and a DC load.

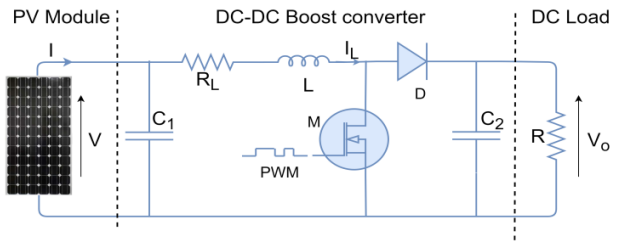

Fig. 1. PV system

PV system parameters applied in this study are as follows:

- I and V denote, respectively, the PV output current and voltage;
- i_L, i_0, V_0 and u denote, respectively, the converter's self-inductance current, load current, load voltage and duty cycle;
- C_1, C_2, L, R_L, R_m and v_d denote, respectively, the input capacitor, output capacitor, boost inductance, resistance of self-inductance, resistance characterizing the loss through the electronic switch (MOSFT) and diode's forward voltage.

PV panel model. According to the electrical circuit of PV panel (Fig. 2), the PV current can be described by [17, 18]:

$$I = n_p I_{ph} - n_p I_s \left(\exp\left(\frac{q(V + IR_s)}{AkT} \right) - 1 \right) - \frac{V + IR_s}{R_{sh}}, \quad (1)$$

where I_s is the cell saturation current in the dark; I_{ph} is the light-generated current; R_{sh} and R_s are the shunt and the cell series resistances respectively; q, k, T, n_p, A are, respectively, the electron charge, Boltzmann constant ($1.38 \cdot 10^{-23}$ J/K), cell temperature, number of parallel solar cells and the ideal factor.

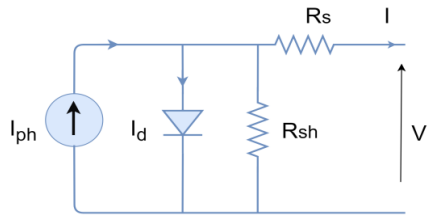

Fig. 2. Electrical equivalent model of PV module

Equation (2) describes the light-generated current I_{ph}, which is dependent on cell temperature T and sun irradiation G:

$$I_{ph} = G(I_{sc} + K_I(T - T_r)), \quad (2)$$

where I_{sc} is the cell short-circuit current at $T = 25$ °C and $G = 1$ kW/m^2; K_I, T_r, G are, respectively, the cell's short-circuit current temperature coefficient, cell's reference temperature and solar irradiation.

Conversely, the saturation current is dependent on cell temperature according to the following expression:

$$I_s = I_{rs} \left(\frac{T}{T_r} \right)^3 \exp\left[\frac{qE_g}{kA} \left(\frac{1}{T_r} - \frac{1}{T} \right) \right], \quad (3)$$

where E_g is the band-gap energy of the semiconductor used in the cell; I_{rs} is the reverse saturation current given by:

$$I_{rs} = \frac{I_{sc}}{\exp\left(\frac{qV_{oc}}{n_s kAT} \right) - 1}, \quad (4)$$

where V_{oc} is the open-circuit voltage.

The considered PV panel is simulated using the MATLAB/Simulink model illustrated in Fig. 3 with the values provided in Table 1. The PV panel is composed of 36 cells, as shown in Fig. 4.

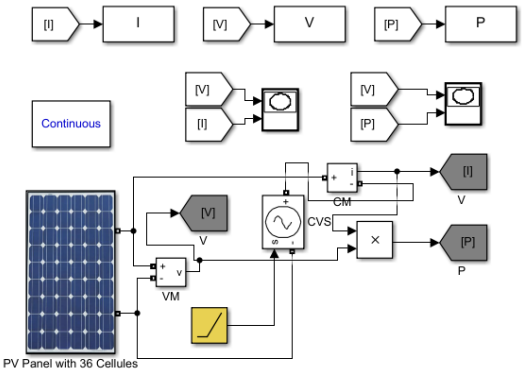

Fig. 3. Simulink model of PV panel

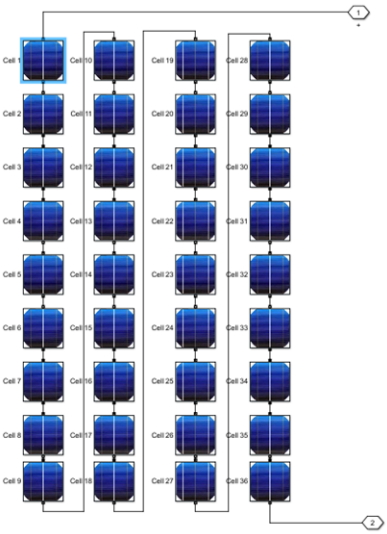

Fig. 4. Simulink model of PV panel cells

Table 1

PV panel parameters

Parameter	Value
Ideal factor of PV cell A, V	1.1
Shunt resistance R_{sh}, Ω	360
Cells connected in series n_s	36
Number of module in parallel n_p	1
Series resistance R_s, Ω	0.18
Temperature reference T_0, K	298
Irradiation reference G_0, W/m^2	100
Nominal short-circuit current I_{scn}, A	3.8
Open-circuit voltage V_{oc}, V	21.6

P-V characteristic (Fig. 5) shows the significant impact of solar irradiation and cell temperature on the fluctuation of the PV module's maximum power $P_{\max}$, which translates to an ideal PV output voltage $V_{\max} = V_{mpp}$. On the other hand, when the PV module is partially shaded, it gives rise to the occurrence of multiple operating points on its P-V characteristic plot.

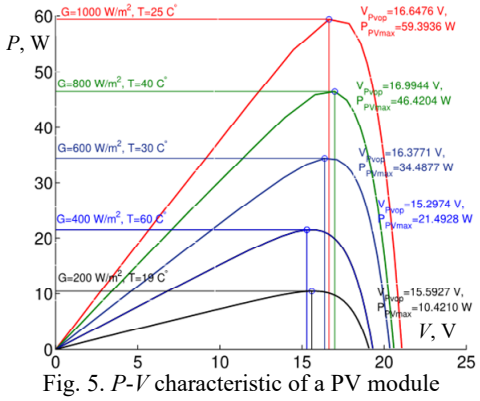

Fig. 5. P-V characteristic of a PV module

DC-DC boost converter model. The dynamic model of DC-DC boost converter can be described as [17]:

$$\begin{cases} \dot{i}_L = -\dfrac{R_L}{L} i_L + \dfrac{1}{L} V - \left(\dfrac{1-u}{L}\right)\left(V_0 + v_d - R_m i_L\right); \\ \dot{V} = -\dfrac{1}{C_1} i_L + \dfrac{1}{C_1} I. \end{cases}, \quad (5)$$

By using (5) and adding a new state, such as $\dot{u} = u_{pv}$, the PV system can be described as:

$$\dot{x}(t) = f(x(t)) + Bu(t) + \eta(t), \quad (6)$$

where

$$f(x(t)) = \begin{bmatrix} -\dfrac{R_L}{L} i_L + \dfrac{1}{L} V - \left(\dfrac{1-u}{L}\right)\left(\dfrac{V_0 + v_d - R_m i_L}{L} u_{pv}\right) \\ -\dfrac{1}{C_1} i_L \\ 0 \end{bmatrix};$$

$$x = \begin{bmatrix} i_L \\ V \\ u_{pv} \end{bmatrix}; \quad B = \begin{bmatrix} 0 \\ 0 \\ 1 \end{bmatrix}; \quad \eta = \begin{bmatrix} -\dfrac{V_0 + v_d}{L} \\ -\dfrac{1}{C_1} I \\ u_{pv} \end{bmatrix}.$$

The considered boost converter parameters are given in Table 2.

Table 2

Boost converter parameters

Parameter	Value
Output capacitor C_1, μF	50
Input capacitor C_2, μF	220
Resistance of self-inductance R_L, Ω	0.5
Resistance of IGBT characterizing R_m, Ω	0.05
Load resistance R, Ω	35
Inductor L, μH	180
Diode's forward voltage v_d, V	1.9

Proposed GMPPT method. The purpose of this study is to design a feedback controller using T-S fuzzy models and ANFIS technique that permit to maximize the output power of the PV Panel. The primary objective is to ensure that the PV system states follow $x = [i_L \;\; V \;\; u_{pv}]^T$ precisely a desired reference $x_d = [i_{Ld} \;\; V_d \;\; u_{pvd}]^T$ regardless of varying weather conditions and partial shading. The initial stage involves designing a T-S fuzzy controller using the nonlinear mathematical model of the PV system. Subsequently, a desirable reference model and a nonlinear tracking controller are determined using a maximum voltage $V_{\max} = V_{mpp}$ which can be determined using an ANFIS. Consequently, the control scheme depicted in Fig. 6 is proposed.

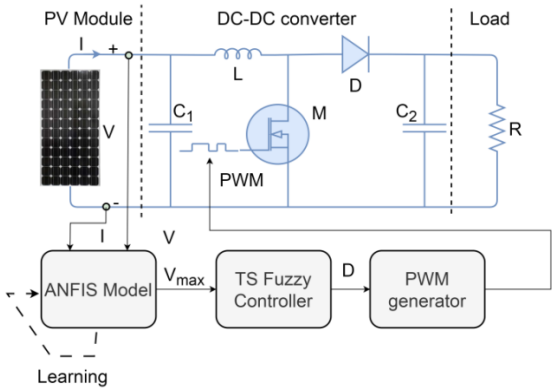

Fig .6. Control scheme of proposed GMPPT method

ANFIS design. The implementation of an ANFIS for the prediction of the maximum voltage is illustrated in Fig 7.

Simulink/SimPower models of the PV module operating in diverse climatic conditions and under various partial shading, scenarios are employed to create the training dataset for the ANFIS. These datasets encompass predictor inputs and corresponding desired output values. The system

involves two inputs, the PV voltage and PV current and a single output representing the maximum PV voltage which corresponds to the actual maximum power point. The ANFIS network formulates fuzzy rules based on a provided input-output dataset, utilizing suitable membership functions whose shape parameters are adjusted in the learning phase. The training process employs a hybrid learning method that integrates the least squares approach with the back-propagation gradient descent algorithm.

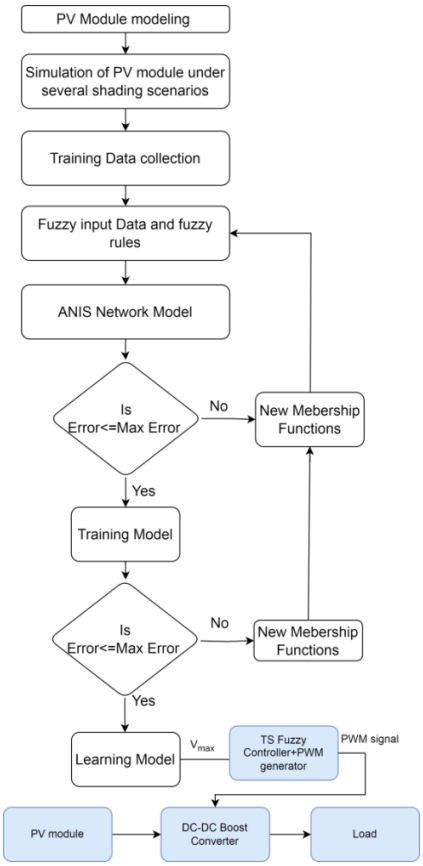

Fig. 7. ANFIS flowchart

Fuzzy modeling of the PV system. To design the feedback T-S controller, the nonlinear system given by (6) is converted into a T-S fuzzy model. This transformation is achieved by considering the converter inductance current i_L and the load voltage V_0 as decision variables. Consequently, the following state space representation is produced:

$$\dot{x}(t) = A(i_L, V_0)x(t) + Bu(t) + \eta(t), \tag{7}$$

where:

$$A = \begin{bmatrix} -\frac{R_L}{L} & \frac{1}{L} & \frac{V_0 + v_d - R_m i_L}{L} \\ -\frac{1}{C_1} & 0 & 0 \\ 0 & 0 & 0 \end{bmatrix}, B = \begin{bmatrix} 0 \\ 0 \\ 1 \end{bmatrix}, \eta = \begin{bmatrix} -\frac{V_0 + v_d}{L} \\ \frac{1}{C_1} i_{pv} \\ 0 \end{bmatrix}.$$

Assuming that the output load voltage and the boost inductance current are bounded as:

$$\underline{i}_L \le i_L \le \bar{i}_L, \quad \underline{V}_0 \le V_0 \le \overline{V}_0, \tag{8}$$

and using the nonlinearity transformation sector approach [19], the mathematical model of the PV system (7) can be given by a fuzzy models with $r = 2^n = 2^2 = 4$ If-Then rules, as follows: Rule i: If $z_1(t)$ is F_{1i} and $z_2(t)$ is F_{2i}. Then

$$\dot{x}(t) = A_i x(t) + B_i u(t) + \eta(t), \; i = 1,...,r,$$

where $z_1 = i_L$ and $z_2 = V_0$ are the premise variables, F_{11}, F_{12}, F_{21}, F_{22} are the membership functions given by:

$$\begin{cases} F_{11}(i_L) = \dfrac{i_L(t) - \underline{i}_L}{\bar{i}_L(t) - \underline{i}_L}, \quad F_{12}(i_L) = 1 - F_{11}(i_L); \\ F_{21}(V_0) = \dfrac{V_0(t) - \underline{V}_0}{\overline{V}_0(t) - \underline{V}_0}, \quad F_{22}(V_0) = 1 - F_{21}(V_0). \end{cases} \tag{9}$$

The sub-matrices are defined as:

$$A_1 = \begin{bmatrix} -\frac{R_L}{L} & \frac{1}{L} & \frac{\overline{V}_0 + v_d - R_m \underline{i}_L}{L} \\ -\frac{1}{C_1} & 0 & 0 \\ 0 & 0 & 0 \end{bmatrix}, A_2 = \begin{bmatrix} -\frac{R_L}{L} & \frac{1}{L} & \frac{\underline{V}_0 + v_d - R_m \underline{i}_L}{L} \\ -\frac{1}{C_1} & 0 & 0 \\ 0 & 0 & 0 \end{bmatrix},$$

$$A_3 = \begin{bmatrix} -\frac{R_L}{L} & \frac{1}{L} & \frac{\overline{V}_0 + v_d - R_m \underline{i}_L}{L} \\ -\frac{1}{C_1} & 0 & 0 \\ 0 & 0 & 0 \end{bmatrix}, A_4 = \begin{bmatrix} -\frac{R_L}{L} & \frac{1}{L} & \frac{\underline{V}_0 + v_d - R_m \underline{i}_L}{L} \\ -\frac{1}{C_1} & 0 & 0 \\ 0 & 0 & 0 \end{bmatrix},$$

$$B_1 = B_2 = B_3 = B_4 = \begin{bmatrix} 0 \\ 0 \\ 1 \end{bmatrix}.$$

The overall output of the T-S fuzzy model can be given by:

$$\dot{x}(t) = \sum_{i=1}^{r} h_i(z(t))(A_i x(t) + B_i u(t)) + \eta(t), \tag{10}$$

where $h_i(z) = w_i(z) \Big/ \sum_{i=1}^{r} w_j(z), w_i(z) = \prod_{j=1}^{n} F_{ij}(z_j)$ for all $t > 0$, $h_i(z) \ge 0$ and $\sum_{i=1}^{r} h_i(z) = 1$.

T-S fuzzy controller gains. The aim is to develop a feedback fuzzy controller that can steer the state of the PV system, denoted as $x(t)$, to closely match a reference model $x_d(t)$. Subsequently, the feedback tracking control must adhere to the following conditions:

$$x(t) - x_d(t) \to 0 \text{ as } t \to \infty. \tag{11}$$

The derivative of the tracking error $\dot{\tilde{x}}(t)$ can be defined as:

$$\dot{\tilde{x}}(t) = \dot{x}(t) - \dot{x}_d(t). \tag{12}$$

By substituting (10) in (12) and adding the term $\sum_{i=1}^{r} h_i(z) A_i(x(t) - x_d(t))$, equation (12) becomes:

$$\dot{\tilde{x}}(t) = \sum_{i=1}^{r} h_i(z)(A_i \tilde{x} + B_i u + A_i x_d) + \eta(t) - \dot{x}_d(t). \tag{13}$$

Equation (13) can be written as:

$$\dot{\tilde{x}}(t) = \sum_{i=1}^{r} h_i(z(t))(A_i \tilde{x}(t) + B_i \tau_u(t)), \tag{14}$$

where

$$\sum_{i=1}^{r} h_i B_i \tau_u(t) = \sum_{i=1}^{r} h_i(z)(A_i x_d(t) + B_i u(t) + \eta - \dot{x}_d(t)). \tag{15}$$

T-S feedback controllers are developed to solve the control problem as outlined below.

Controller rule i: If $z_1(t)$ is F_{1i} and $z_2(t)$ is F_{2i} Then $\tau_u(t) = -K_i \tilde{x}(t)$.

The final output of the fuzzy controller is given as:

$$\tau_u(t) = -\sum_{i=1}^{r} h_i(z(t)) K_i \tilde{x}(t). \quad (16)$$

By applying T-S control law (16) to model (14), the closed-loop system is represented as:

$$\dot{\tilde{x}}(t) = \sum_{i=1}^{r}\sum_{j=1}^{r} h_i(z(t)) h_j(z(t)) (A_i - B_i K_j) \tilde{x}(t). \quad (17)$$

By letting $G_{ij} = (A_i - B_i K_j)$, equation (17) can be expressed as:

$$\dot{\tilde{x}}(t) = \sum_{i=1}^{r}\sum_{j=1}^{r} h_i(z(t)) h_j(z(t)) G_{ij} \tilde{x}(t). \quad (18)$$

To compute the feedback controller gains K_i, the subsequent theorem is taken into consideration [20].

Theorem: T-S fuzzy system described by (18) is globally asymptotically stable if there exists a matrix $X > 0$, a diagonal matrix Q, matrices M_i and matrices Z_{ij} with: $Z_{ii} = Z_{ii}^T$ and $Z_{ji} = Z_{ij}^T$ for $i \neq j$, such that:

$$\begin{bmatrix} XA_i^T + A_i X - B_i M_i - M_i^T B_i^T + Y_{ii} & XQ^T \\ QX & -X \end{bmatrix} < 0. \quad (19)$$

$$\begin{aligned} & XA_i^T + A_i X + XA_j^T + A_j X - B_i M_j - M_j^T B_i^T \\ & - B_j M_i - M_i^T B_j^T + 2Z_{ij} \le 0, \quad i < j < r. \end{aligned} \quad (20)$$

$$\begin{bmatrix} Z_{11} & Z_{12} & \cdots & Z_{1r} \\ Z_{12} & Z_{22} & \cdots & Z_{2r} \\ \vdots & \ddots & \vdots & \vdots \\ Z_{1r} & Z_{2r} & \cdots & Z_{rr} \end{bmatrix} \equiv \tilde{z} > 0. \quad (21)$$

The feedback controller gains can be extracted as:

$$K_i = M_i X^{-1}. \quad (22)$$

Controller law and reference model. The controller law $u(t)$ and the variables of the desired reference model, represented by $x_d(t)$, can be determined through the utilization of (15), which is restated as:

$$\sum_{i=1}^{r} h_i B_i (u(t) - \tau_u(t)) = -\sum_{i=1}^{r} h_i A_i x_d(t) - \eta(t) + \dot{x}_d(t). \quad (23)$$

Noting that:

$$A(i_L, V_0) = \sum_{i=1}^{r} h_i A_i, \quad B = \sum_{i=1}^{r} h_i B_i. \quad (24)$$

Then, equation (23) can be rewritten as the following compact form:

$$B(u - \tau_u) = -A(i_L, V_0) x_d - \eta + \dot{x}_d. \quad (25)$$

In matrix notation, the equation (25) can be given as:

$$\begin{bmatrix} 0 \\ 0 \\ 1 \end{bmatrix} (u - \tau_u) = -\begin{bmatrix} -\frac{R_L}{L} & \frac{1}{L} & \alpha \\ -\frac{1}{C_1} & 0 & 0 \\ 0 & 0 & 0 \end{bmatrix} \begin{bmatrix} i_d \\ V_d \\ u_d \end{bmatrix} - \begin{bmatrix} -\beta \\ \frac{1}{C_1} i_{pv} \\ 0 \end{bmatrix} + \frac{\mathrm{d}}{\mathrm{d}t} \begin{bmatrix} i_d \\ V_d \\ u_d \end{bmatrix}. \quad (26)$$

where

$$\alpha = \frac{V_0 + V_d - R_m i_L}{L}, \quad \beta = \frac{V_0 + V_d}{L}.$$

It is important to highlight that the optimal reference and the nonlinear controller are calculated based on the optimal voltage reference which corresponds to the maximum voltage $V_d = V_{\max}$. The second equation of (26) implies:

$$i_d(V_d) = i_{pv} - C_1 \dot{V}_d. \quad (27)$$

From the initial equation in (26), it can be inferred that:

$$u_d(V_d) = \frac{1}{\alpha}\left(\frac{R_L}{L} i_d - \frac{1}{L} V_d + \beta + \dot{i}_d\right). \quad (28)$$

The nonlinear tracking control is derived from the third equation in (26), as outlined below:

$$u(V_d) = \dot{u}_d(V_d) + \tau_u. \quad (29)$$

Figure 8 shows the configuration of the proposed MPPT controller and its key components. The first block is dedicated to the calculation of the maximum voltage $V_{\max}$. This computation involves a fuzzy inference system that takes PV voltage V and PV current I measurements as inputs. Next, $V_{\max}$ is utilized by the desired reference block to produce x_d using (27) and (28). Following this, the fuzzy controller generates the fuzzy control signal utilizing (16), derived from the error $e(t)$ between the current and desired states. This generated signal is then utilized by the nonlinear controller block, employing (29) to produce the ultimate control signal. Further insights into the fuzzy inference system block will be provided in the subsequent section.

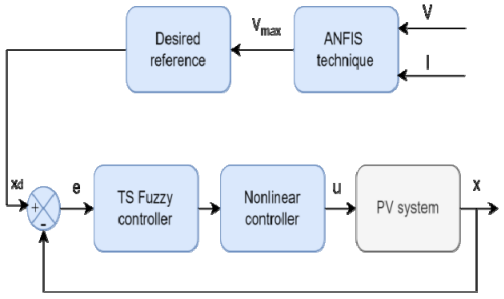

Fig. 8. Diagram of the control strategy

Simulation results. To validate the proposed method's efficacy, simulation tests of the PV system were conducted using the Simulink model (Fig. 9).

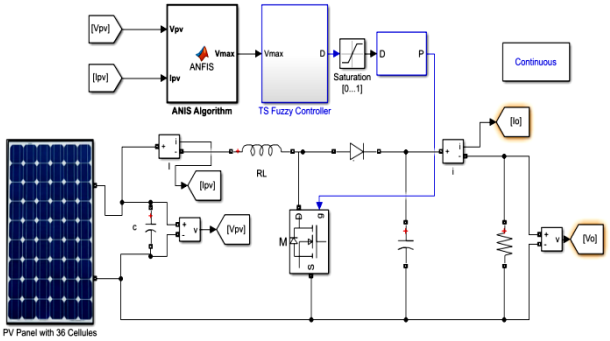

Fig. 9. Simulink model of the proposed control method

The obtained T-S feedback gains are computed as:

$$K_1 = [155.0075 \quad -0.6106 \quad 633.6307];$$
$$K_2 = [92.6114 \quad -0.1194 \quad 570.2396];$$
$$K_3 = [282.7187 \quad -0.4403 \quad 616.0382];$$
$$K_4 = [103.4164 \quad 0.3952 \quad 577.9426].$$

The maximum voltage, which corresponds to the peak power corresponding to the peak power, is calculated using an MPPT algorithm based on the ANFIS algorithm (see Fig. 7). This algorithm relies on a database constructed from the *P-V* characteristic, where fuzzy membership functions model the PV voltage and PV current. This method establishes a fuzzy relationship between these parameters and the maximum voltage.

The initial simulation is conducted under diverse conditions with variable solar radiance and temperature, assuming temperatures and irradiation levels as illustrated in Fig. 10,*a* and Fig. 10,*b*, respectively.

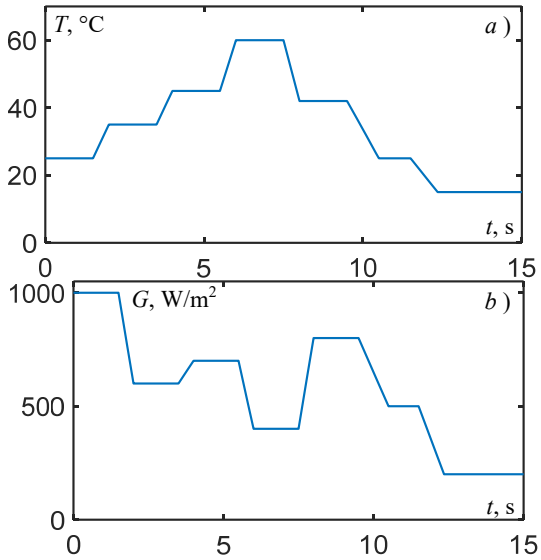

Fig. 10. Temperature (*a*) and radiance (*b*) profiles for the first test

Figures 11,*a*,*b* display the responses of PV voltage and PV power, respectively, while Fig. 11,*c*,*d* depict the responses of the boost converter current and control signal. Notably, the steady states align precisely, with the desired trajectories, remaining unaffected by variations in solar irradiation and cell temperature. This precision in tracking optimal paths contributes significantly to the enhanced extraction of available solar power and the overall performance of the system.

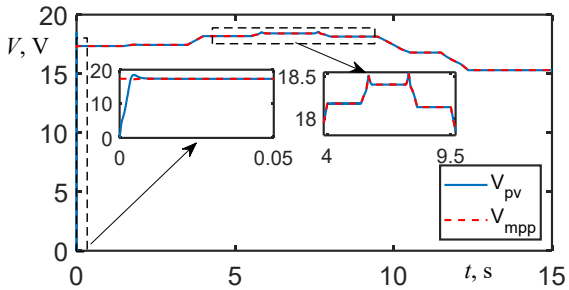

a) PV output voltage

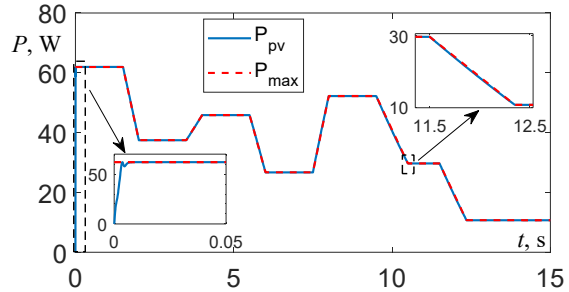

b) PV output power

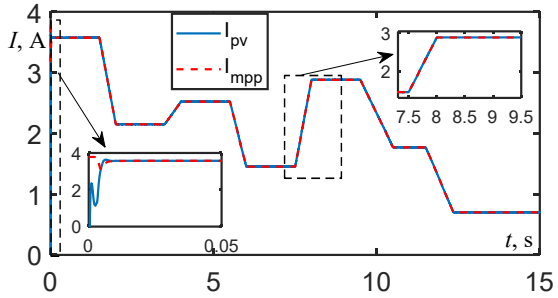

c) Inductance current of boost converter

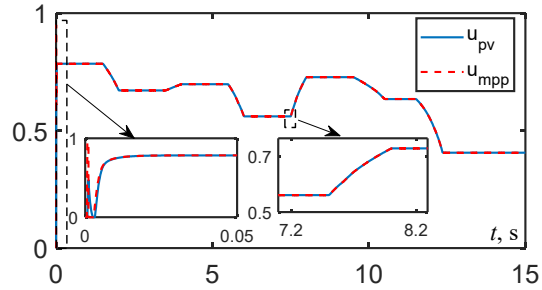

d) Duty cycle

Fig. 11.Simulation results for various atmospheric conditions

The second test involves maintaining a constant temperature while varying irradiation levels as shown in Fig. 12,*a*. The corresponding response of the output power is depicted in Fig. 12,*b*. One can clearly see that the steady states of the system exactly follow the optimal trajectories and remain consistent despite in cell temperature and sun irradiation. The precision with which the system stays on the best courses is critical to optimizing solar energy use and raising the overall system's efficiency.

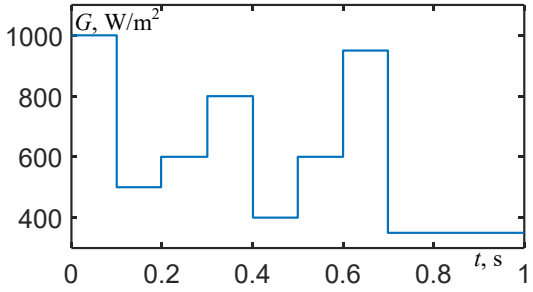

a) Irradiation profile

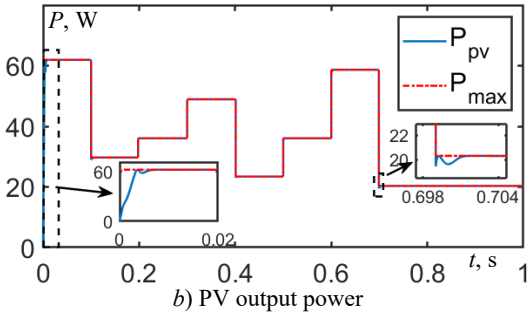

b) PV output power

Fig. 12. Simulation results for sudden change of atmospheric conditions

The third test is conducted under partial shading conditions for a PV panel consisting of 36 cells, with 4 cells shaded, maintaining a constant temperature of $T = 25$ °C and solar irradiation of $G = 1000$ W/m². *P-V* characteristic curve reveals 2 maximum power points: a local maximum of 29.91 W and a global maximum of 52.76 W (Fig. 13,*a*). To assess its performance, the proposed fuzzy method is

compared to conventional methods such as P&O, IncCond, and Particle Swarm Optimization (PSO). Figure 13,*b* presents the responses of the PV output power under partial shading conditions.

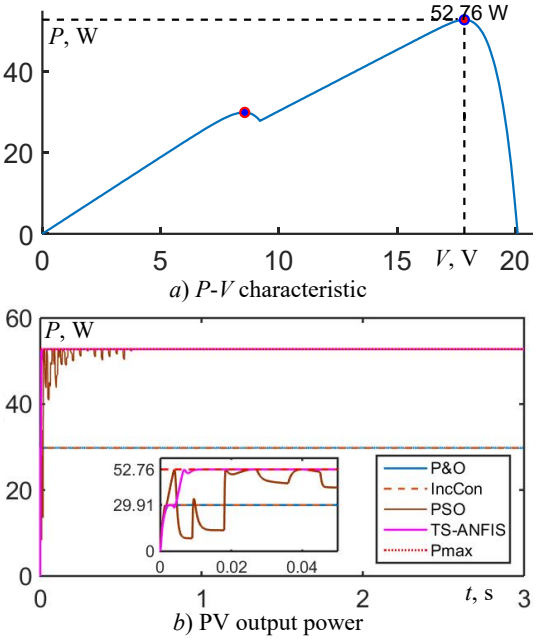

Fig. 13. Simulation results for the third test

One can clearly see that the PSO as well as the proposed methods can identify the global maximum amid various local maxima and quickly stabilize at the maximum global. However, the proposed controller exhibits a rapid response time, efficiently locating and maintaining the global maximum without oscillations. Moreover, conventional methods such as P&O and IncCond tend to stabilize at the minimum power.

The fourth test is conducted under partial shading conditions for a PV panel consisting of 36 cells, with 8 cells shaded, maintaining a constant temperature of $T = 25$ °C and solar irradiation of G = 1000 W/m². P-V characteristic curve reveals 3 maximum power points, including 2 local maxima of 37.86 W and 21.37 W, along with a global maximum of 40.86 W (Fig. 14). Performance evaluation involves a comparison of the proposed fuzzy method with well-known methods such as P&O, IncCond and PSO.

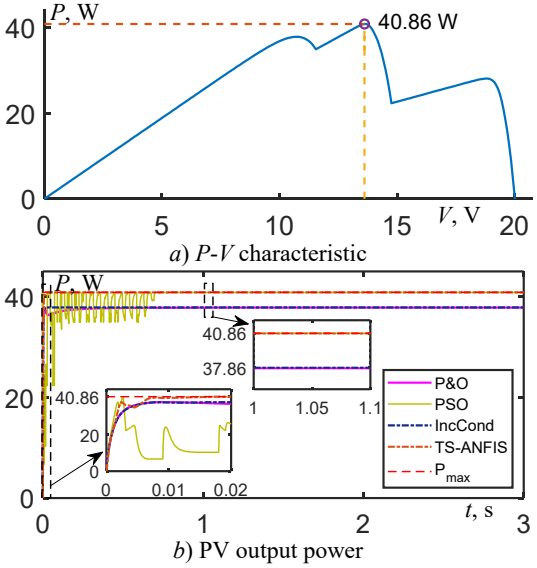

Fig. 14. Simulation results for the fourth test

Simulation tests confirm that the developed MPPT-based controller effectively guides the steady states to closely match the optimal operating points, displaying minimal oscillation. Conversely, the PV system responses under the compared methods exhibit notable fluctuations across different states.

Additionally, the performance of the proposed and comparative methods is evaluated through many indexes such as root mean square error, MPPT energetic efficiency, and MPPT energetic error.

The root mean square error is defined as:

$$E_{rms} = \sqrt{\frac{\sum_{i=1}^{N}\left(P_{pv,i} - P_{\max,i}\right)^2}{N}}. \qquad (30)$$

The static efficiency:

$$\eta = \left(\frac{P_{pv}}{V_{\max}}\right)\cdot 100. \qquad (31)$$

The relative tracking error:

$$\varepsilon = \left(\frac{P_{pv}}{V_{\max}}\right) - 1. \qquad (32)$$

The obtained indexes for the proposed and compared methods are summarized in Table 3.

Table 3

Comparison of different MPPT methods

Index	P&O	InCond	PSO	Proposed
E_{rms}	0.2891	0.2182	0.0575	0.0215
η	46.2568	46.8910	97.1906	98.1256
e	5.2918	5.3109	2.8094	1.0295

This comparative study demonstrates the effectiveness of the proposed control strategy in overcoming the limitations associated in traditional controllers. It is demonstrates also that the proposed controller delivers a faster dynamic response, significantly reduced oscillation around the maximum power point, and overall superior performance.

Conclusions. This paper presents a highly effective Takagi-Sugeno fuzzy controller for global maximum power point tracking in PV conversion systems. This controller demonstrates the capability to guide the PV system in swiftly tracking a desired reference model with minimal oscillations during rapid weather changes and under partial shading conditions.

The desired reference model is determined by the ANFIS algorithm based on the maximum voltage. Fuzzy controller gains are computed according to specific conditions shown in linear matrix inequalities and are determined using optimization tools. Simulation results, alongside comparisons to classic Incremental Conductance, Perturb & Observe and Particle Swarm Optimization algorithms, demonstrate the effectiveness of the proposed fuzzy tracking control scheme in managing the PV system across various operating conditions. Addressing practical implementation and robustness concerns remains a focus for future research endeavors.

Conflict of interest. The authors declare that they have no conflicts of interest.

REFERENCES

1. Chen X.H., Tee K., Elnahass M., Ahmed R. Assessing the environmental impacts of renewable energy sources: A case study on air pollution and carbon emissions in China. *Journal of Environmental*

Management, 2023, vol. 345, art. no. 118525. doi: https://doi.org/10.1016/j.jenvman.2023.118525.
2. Osman A.I., Chen L., Yang M., Msigwa G., Farghali M., Fawzy S., Rooney D.W., Yap P.-S. Cost, environmental impact, and resilience of renewable energy under a changing climate: a review. *Environmental Chemistry Letters*, 2023, vol. 21, no. 2, pp. 741-764. doi: https://doi.org/10.1007/s10311-022-01532-8.
3. Youcef H., Touhami G., Omar O., Essama G.A., Slimane L. Sliding Mode based PSO MPPT for Solar PV System. *Przeglad Elektrotechniczny*, 2024, no. 1, pp. 86-90. doi: https://doi.org/10.15199/48.2024.01.18.
4. Juma'a H.G., Atyia T.H. Design a 91-Multilevel Inverter Circuit Using Solar PV System Sources. *Przeglad Elektrotechniczny*, 2023, no. 11, pp. 127-133. doi: https://doi.org/10.15199/48.2023.11.22.
5. Paquianadin V., Navin Sam K., Koperundevi G. Maximizing solar photovoltaic system efficiency by multivariate linear regression based maximum power point tracking using machine learning. *Electrical Engineering & Electromechanics*, 2024, no. 1, pp. 77-82. doi: https://doi.org/10.20998/2074-272X.2024.1.10.
6. Guiza D., Ounnas D., Soufi Y., Bouden A., Maamri M. Implementation of Modified Perturb and Observe Based MPPT Algorithm for Photovoltaic System. *2019 1st International Conference on Sustainable Renewable Energy Systems and Applications (ICSRESA)*, 2019, pp. 1-6. doi: https://doi.org/10.1109/ICSRESA49121.2019.9182483.
7. Zerzouri N., Ben Si Ali N., Benalia N. A maximum power point tracking of a photovoltaic system connected to a three-phase grid using a variable step size perturb and observe algorithm. *Electrical Engineering & Electromechanics*, 2023, vol. 5, pp. 37-46. doi: https://doi.org/10.20998/2074-272X.2023.5.06.
8. Dhaouadi G., Djamel O., Youcef S., Salah C. Implementation of Incremental Conductance Based MPPT Algorithm for Photovoltaic System. *2019 4th International Conference on Power Electronics and Their Applications (ICPEA)*, 2019, pp. 1-5. doi: https://doi.org/10.1109/ICPEA1.2019.8911186.
9. Louarem S., Kebbab F.Z., Salhi H., Nouri H. A comparative study of maximum power point tracking techniques for a photovoltaic grid-connected system. *Electrical Engineering & Electromechanics*, 2022, no. 4, pp. 27-33. doi: https://doi.org/10.20998/2074-272X.2022.4.04.
10. Jately V., Azzopardi B., Joshi J., Balaji Venkateswaran V., Sharma A., Arora S. Experimental analysis of hill-climbing MPPT algorithms under low irradiance levels. *Renewable and Sustainable Energy Reviews*, 2021, vol. 150, art. no. 111467. doi: https://doi.org/10.1016/j.rser.2021.111467.
11. Ounnas D., Guiza D., Soufi Y., Maamri M. Design and Hardware Implementation of Modified Incremental Conductance Algorithm for Photovoltaic System. *Advances in Electrical and Electronic Engineering*, 2021, vol. 19, no. 2, pp. 100-111. doi: https://doi.org/10.15598/aeee.v19i2.3881.
12. Wang Q., Chang X. Maximum Power Point Tracking of PV System Under Partial Shading Conditions Based on TSO-IP&O Algorithm. *2023 3rd International Conference on Energy, Power and Electrical Engineering (EPEE)*, 2023, pp. 155-159. doi: https://doi.org/10.1109/EPEE59859.2023.10351794.
13. Chaibi R., Bachtiri R.E., Hammoumi K.E., Yagoubi M. Photovoltaic System's MPPT Under Partial Shading Using T-S Fuzzy Robust Control. *IFAC-PapersOnLine*, 2022, vol. 55, no. 12, pp. 214-221. doi: https://doi.org/10.1016/j.ifacol.2022.07.314.
14. Moussaoui L., Aouaouda S., Rouaibia R. Fault tolerant control of a permanent magnet synchronous machine using multiple constraints Takagi-Sugeno approach. *Electrical Engineering & Electromechanics*, 2022, no. 6, pp. 22-27. doi: https://doi.org/10.20998/2074-272X.2022.6.04.
15. Guiza D., Soufi Y., Ounnas D., Metatla A. Design and Implementation of Takagi-Sugeno Fuzzy Tracking Control for a DC-DC Buck Converter. *Advances in Electrical and Electronic Engineering*, 2019, vol. 17, no. 3, pp. 234-243. doi: https://doi.org/10.15598/aeee.v17i3.3126.
16. Sekhar P.C., Mishra S. Takagi–Sugeno fuzzy-based incremental conductance algorithm for maximum power point tracking of a photovoltaic generating system. *IET Renewable Power Generation*, 2014, vol. 8, no. 8, pp. 900-914. doi: https://doi.org/10.1049/iet-rpg.2013.0219.
17. Ounnas D., Ramdani M., Chenikher S., Bouktir T. An Efficient Maximum Power Point Tracking Controller for Photovoltaic Systems Using Takagi–Sugeno Fuzzy Models. *Arabian Journal for Science and Engineering*, 2017, vol. 42, no. 12, pp. 4971-4982. doi: https://doi.org/10.1007/s13369-017-2532-0.
18. Kahsay A.H., Regulski P., Derugo P. AI-based control techniques for maximum power point tracking of photovoltaic systems using a boost converter. *Przeglad Elektrotechniczny*, 2023, no. 11, pp. 1-6. doi: https://doi.org/10.15199/48.2023.11.01.
19. Ohtake H., Tanaka K., Wang H.O. Fuzzy modeling via sector nonlinearity concept. *Integrated Computer-Aided Engineering*, 2003, vol. 10, no. 4, pp. 333-341. doi: https://doi.org/10.3233/ICA-2003-10404.
20. Ounnas D., Ramdani M., Chenikher S., Bouktir T. Optimal reference model based fuzzy tracking control for wind energy conversion system. *International Journal of Renewable Energy Research*, 2016, vol. 6, no. 3, pp. 1129-1136. doi: https://doi.org/10.20508/ijrer.v6i3.4258.g6896.

Received 25.08.2024
Accepted 24.10.2024
Published 02.03.2025

N. Hadjidj[1]*, PhD,*
M. Benbrahim[1]*, PhD, Associate Professor,*
D. Ounnas[2]*, PhD, Associate Professor,*
L.H. Mouss[1]*, Professor,*
[1] Industrial Engineering Department,
Laboratory of Automation and Manufacturing Engineering,
University of Batna 2, Algeria,
e-mail: n.hadjidj@univ-batna2.dz (Corresponding Author);
m.benbrahim@univ-batna2.dz;
h.mouss@univ-batna2.dz
[2] LABGET Laboratory, Department of Electrical Engineering,
Faculty of Technology, University of Tebessa, Algeria,
e-mail: djamel.ounnas@univ-tebessa.dz

How to cite this article:
Hadjidj N., Benbrahim M., Ounnas D., Mouss L.H. Global maximum power point tracking method for photovoltaic systems using Takagi-Sugeno fuzzy models and ANFIS approach. *Electrical Engineering & Electromechanics*, 2025, no. 2, pp. 31-38. doi: https://doi.org/10.20998/2074-272X.2025.2.05